# State-of-the-art modeling of impurity transport in stellarators


J. M. García-Regaña.

CIEMAT


XVIII European Fusion Theory Conference

Ghent, 7 October 2019

- **CIEMAT** J. L. Velasco, I. Calvo, A. González-Jerez, T. Estrada, D. Carralero, E. Sánchez, A. Alonso and TJ-II Team.
- **PPPL** A. Mollén, N. Pablant.
- **U. Oxford** M. Barnes and F. Parra.
- **Max Planck IPP** H. Smith, R. Kleiber, J. Alcusón, A. Langenberg, P. Xanthopoulos, A. Zocco.
- **NIFS** S. Satake and K. Fujita.
- and **W7-X team**.

- Stellarators count with a number of situations with reduced impurity core confinement that **standard neoclassical modeling** have not successfully modeled.
- These situations are best exemplified by the **LHD impurity hole** plasmas (left figure), the **high-density-H (HDH) mode W7-AS** plasma (right fig. $\diamond$).

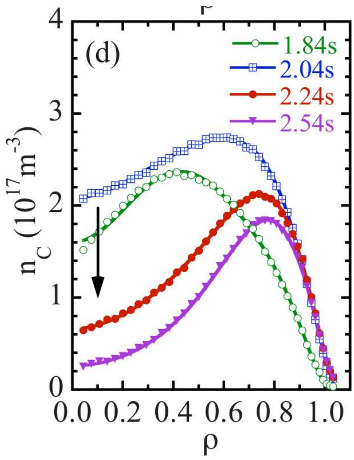


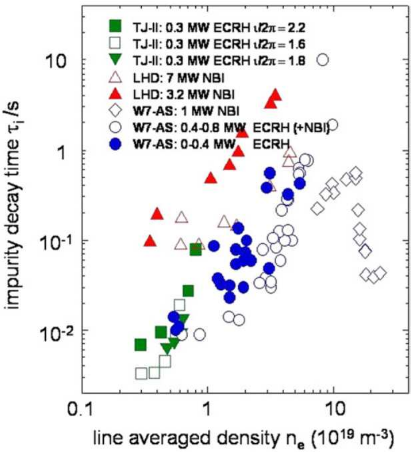


[Ida PoP'11] (left) ; [McCormick PRL'02] (right)

**Standard** neoclassical modelling:

- Radially local *monoenergetic* ($r$ and $v$ are mere parameters) DKES [Hirshman PF'86] based calculations.
- Trucated electric field (only radial, $E_r$) and incompressible form of $E_r \times B$ drift.
- Pitch-angle-scattering collisions, with momentum conservation schemes, of limited application to impurity calculations.

⇒ Recent **intense code development and analytical effort** to improve the modeling of **collisional** impurity transport.

- **Neoclassical radial fluxes** ($\Gamma$) are **not intrinsically ambipolar** in stellarators for $E_r = 0$. $E_r$ is constrained by:

$$\sum_\alpha Z_\alpha e \Gamma_\alpha(E_r) = 0.$$

- Over the flux surfaces **unbalanced charge density** leads the plasma to generate a potential $\varphi_1$ **to preserve quasineutrality**.

### $\varphi_1$ scaling at low $\nu_{*i}$ [Calvo JPP'18]

- In stellarators $\varphi_1 \sim \nu_{*i}^{-1}$ in the $1/\nu$ regime up to constant values reached at either at the $\sqrt{\nu}$-regime (**large** $E_r$) or *superbanana-plateau* regime (**low** $E_r$).
- In tokamaks $\varphi_1 \sim \nu_{*i}$ at low collisionality.
- The $E \times B$ and magnetic drifts become comparable as $Z$ increases:

$$\mathbf{v}_m \cdot \nabla r \sim \mathbf{v}_{E1} \cdot \nabla r.$$

- The electrostatic and magnetic trapping become comparable as $Z$ increases:

$$\mu \nabla_\parallel B \sim Ze \nabla_\parallel \Phi_1.$$

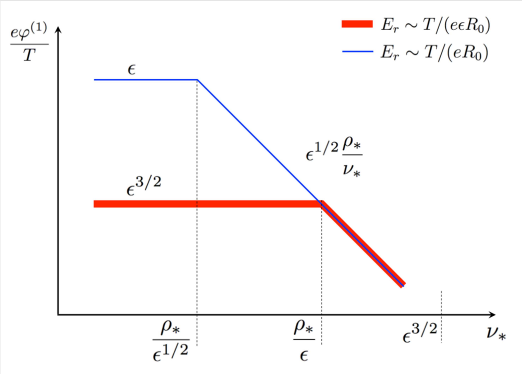

- Impact of $\varphi_1$ on $\Gamma_Z$ confirmed for $e\varphi_1/T_i \lesssim 0.05$ and low-$Z$ impurities like $C^{6+}$ [Regaña PPCF'13, Regaña NF'17].
- The *phase* of $f_{1Z}$ respect to $(\mathbf{v}_m + \mathbf{v}_{E1}) \cdot \nabla r$ underlies the impact of $\varphi_1$ on the $\Gamma_Z$.

$$\Gamma_Z = \left\langle \int f_{1Z}(\mathbf{v}_m + \mathbf{v}_{E1}) \cdot \nabla r d^3 v \right\rangle$$

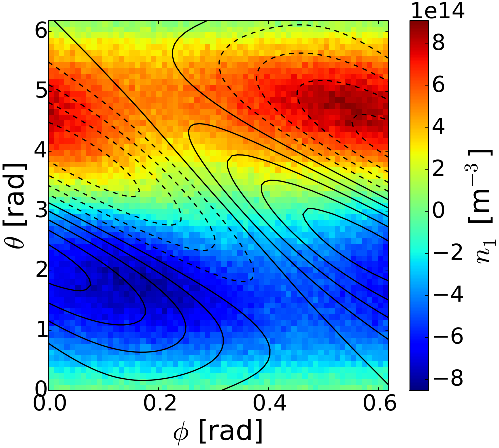


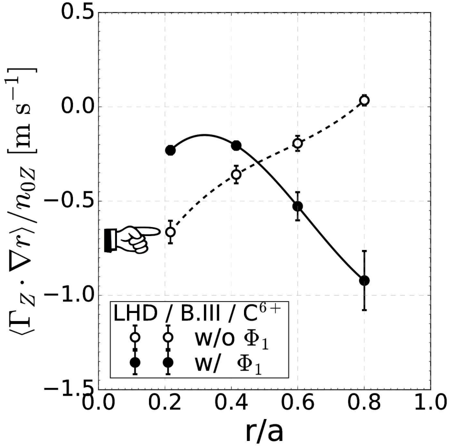


- **Without** $\varphi_1$.
- $\mathbf{v}_m \cdot \nabla r$ and $n_{1Z}$ for $C^{6+}$
- **Inward radial drift** (dashed) overlap **high** $C^{6+}$ **density regions**.

$\Rightarrow$ **Stronger inward flux**

- Impact of $\varphi_1$ on $\Gamma_Z$ confirmed for $e\varphi_1/T_i \lesssim 0.05$ and low-$Z$ impurities like $C^{6+}$ [Regaña PPCF'13, Regaña NF'17].
- The *phase* of $f_{1Z}$ respect to $(\mathbf{v}_m + \mathbf{v}_{E1}) \cdot \nabla r$ underlies the impact of $\varphi_1$ on the $\Gamma_Z$.

$$\Gamma_Z = \left\langle \int f_{1Z}(\mathbf{v}_m + \mathbf{v}_{E1}) \cdot \nabla r d^3 v \right\rangle$$

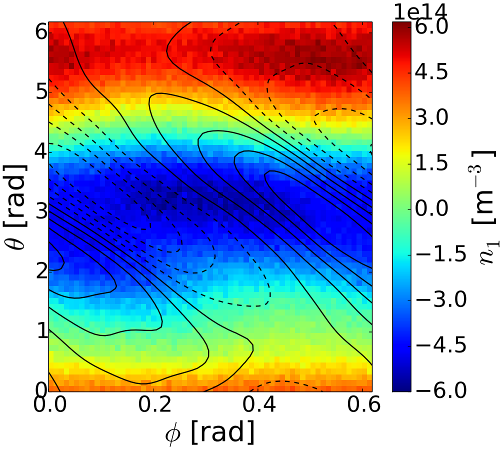


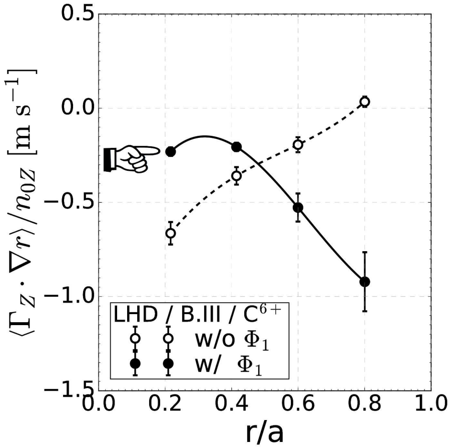


- **Without** $\varphi_1$.
- $(\mathbf{v}_m + \mathbf{v}_{E1}) \cdot \nabla r$ and $n_{1Z}$ for $C^{6+}$
- Radial (inward or outward) drifts do **not preferentially overlap** high or low $C^{6+}$ density regions.

$\Rightarrow$ **Weakier inward flux**

# What to improve respect to first EUTERPE simulations of $\varphi_1$ and $\Gamma_Z$ [Regaña NF'17]?

- EUTERPE is a $\delta f$ PIC code, radially global on its gyrokinetic version.
- In this presentation we use the **radially local <u>neoclassical version</u>**.
- It solves

$$\frac{\partial f_1}{\partial t} + \dot{\mathbf{R}}^0 \cdot \nabla f_1 + \dot{v}_{\|}^0 \frac{\partial f_1}{\partial v_{\|}} = -f_{\mathrm{M}} \left( \mathbf{v}_m + \mathbf{v}_{E1} \right) \cdot \nabla r \left[ \frac{n'}{n} + \frac{Ze}{T} E_r + \left( \frac{mv^2}{2T} - \frac{3}{2} + \frac{Ze}{T} \Phi_1 \right) \frac{T'}{T} \right] + C(f).$$

$$\Phi_1 = \frac{T_e}{e} \left( n_{0e} + n_{0i} \frac{T_e}{T_i} \right)^{-1} \left( n_{1i} - n_{1e} \right).$$

1. The guiding center trajectory $\dot{\mathbf{R}}^0$ does not retain the **magnetic drift** (neither the component accross the surface nor the tangential component $\mathbf{v}_m \cdot \nabla \alpha$).

$\Rightarrow$ Neglecting $\mathbf{v}_m \cdot \nabla \alpha \rightarrow$ unrealistic situation with vanishing drift over flux surface when $E_r = 0$.

$\Rightarrow$ Unphysically large size of $f_1$ and its moments (including $\varphi_1$) in the vicinity of $E_r = 0$.

2. The collision operator used included only **pitch-angle-scattering**, with questionable application to moderate to high collisional impurities.
3. Integration **timestep** has to be **reduced** a factor of $O(\sqrt{m_e/m_i})$ when kinetic electrons need to be considered.

## KNOSOS [Velasco (2019) arXiv:1908.11615]

- **Bounce-averaged** local neoclassical code that, following [Calvo, PPCF'17], consistently solves at low collisionality and arbitrary geometry:

  **Drift kinetic equation** (DKE) $\rightarrow g_b$ and fluxes like $\Gamma$ and $Q$;

  **Ambipolarity condition** $\rightarrow E_r$;

  **Quasi-neutrality** equation $\rightarrow \varphi_1$;
- It includes analytically exact **tangential magnetic drift** $\mathbf{v}_m \cdot \nabla\alpha$.
- O(1) min. of computing time per flux surface, $\times 2$ if kinetic electrons are included.

**Effect of the $\mathbf{v}_m \cdot \nabla\alpha$ on $\varphi_1$ and benchmark for an LHD case**

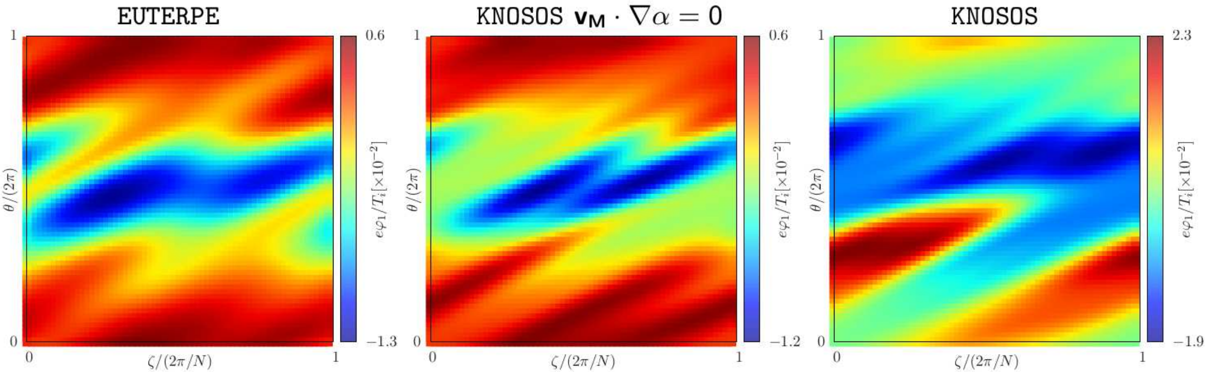


$g_b$ is the departure of distribution function from a Maxwellian; $\alpha = \theta - \iota\zeta$ labels magnetic field lines;

- Alternatively, the full drift trajectories can be integrated, i.e. perform a radially global simulation.
- FORTEC-3D [Satake PFR'06], a PIC $\delta f$ radially global (5D) code, has found corrections to EUTERPE's $\varphi_1$ as those found by KNOSOS in the situations where $\mathbf{v}_m \cdot \nabla\alpha$ can be important [Fujita PFR'19].

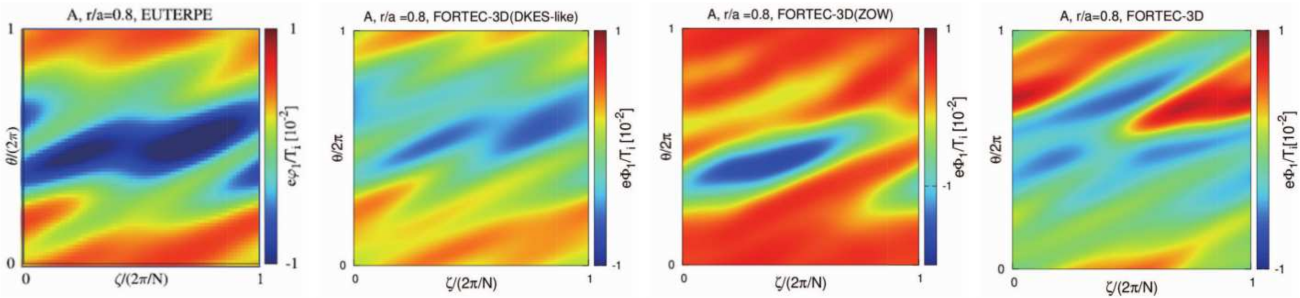

# The importance of the collision operator and the code SFINCS

- The linearized impurity-main ion collision can be $\sqrt{m_i/m_Z}$-expanded to see that three main pieces controls $\Gamma_Z$: I) pitch-angle and energy diffusion; II) friction against main ions; III) main ion pressure anisotropy [Mollén PoP'15].

$$C^{l}_{Zi}\left[F_{1Z};h_i\right]=\overbrace{\frac{\nu_{Zi}T}{m_Z}\nabla_v\cdot\left[F_{MZ}\nabla_v\left(\frac{F_{Z1}}{F_{MZ}}\right)\right]}^{(I)}+\overbrace{\frac{\nu_{Zi}m_Z}{T}Av_{\parallel}}^{(II)}-\overbrace{\frac{\nu_{Zi}m_Z}{T}\left(\mathrm{tr}(\overleftrightarrow{M})-\frac{m_Z}{T}\overleftrightarrow{M}:\mathbf{vv}\right)}^{(III)}.$$

- (II) and (III) depend on main ion distribution $h_i$ through $A$ and $\overleftrightarrow{M}$.
- (II) is responsible for parallel momentum conservation; (III) can be important in stellarators [Calvo arXiv: 1907.08482, see **P1-05**].

## SFINCS [Landremann PoP'14]

- Local neoclassical (4D) $\delta f$ continuum code that consistently solves, for arbitrary geometry, DKE, ambipolar condition and quasi-neutrality.
- It includes all these effects, as it implements the **linearized Fokker-Planck collision operator**.
- **Multispecies at non-trace concentration**.

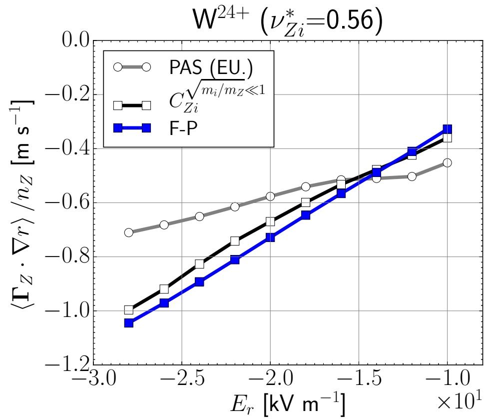


EUTERPE PAS and mass-ratio-expanded collision operator (w/o III) vs. SFINCS .

In the *mixed collisionality regime*:

- When the main ions are low collisional and the impurities are in the Pfirsch-Schlüter regime:

$\rightarrow$ if $\varphi_1 = 0$ the dependence of $\Gamma_Z$ on $E_r$ vanishes. [Helander PRL'17] $\rightarrow$ more likely screening.

$\rightarrow$ if $\varphi_1 \neq 0$ the dependence of $\Gamma_Z$ on $E_r$ is recovered, even at low $\varphi_1$ values [Calvo NF'18, Buller JPP'18].

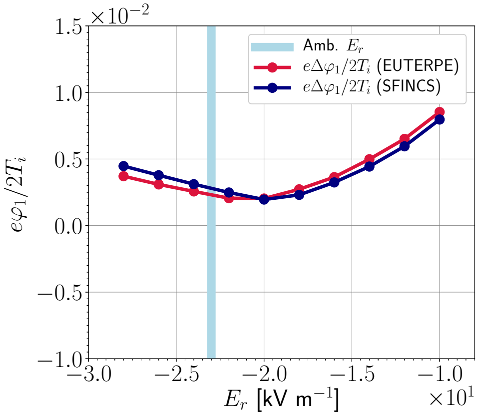


$\Delta\varphi_1 = \varphi_1^{\max} - \varphi_1^{\min}$ for W7-X, $r/a = 0.8$, $T_i = 1.9$ keV, $d_r \log T_i = -6.8$, $T_e = 1.3$ keV, $d_r \log T_e = -6.5$, $n_i = 1.15 \times 10^{20}$ m$^{-3}$ $d_r \log n_i = -5.8$.

# Analytical results: the *mixed-collisionality* regime

**In the *mixed collisionality regime*:**

- When the main ions are low collisional and the impurities are in the Pfirsch-Schlüter regime:

$\rightarrow$ if $\varphi_1 = 0$ the dependence of $\Gamma_Z$ on $E_r$ vanishes. [Helander PRL'17] $\rightarrow$ more likely screening.

$\rightarrow$ if $\varphi_1 \neq 0$ the dependence of $\Gamma_Z$ on $E_r$ is recovered, even at low $\varphi_1$ values [Calvo NF'18, Buller JPP'18].

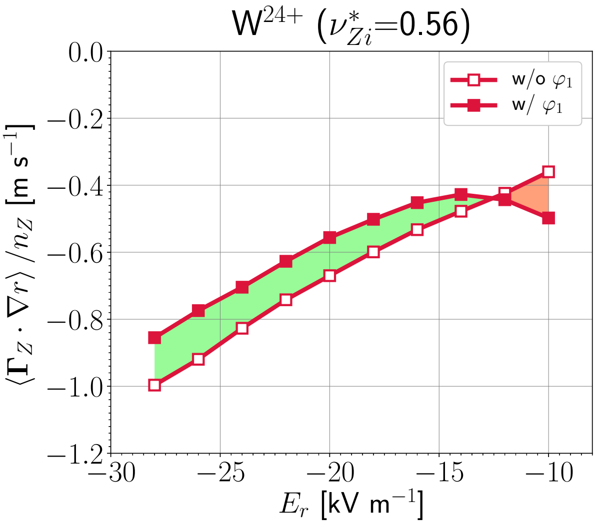


- w/o $\varphi_1$: The monotonic flux **dependence on** $E_r$ weakens, or equivalently $\Gamma_Z(E_r)$ flattens.
- w/ $\varphi_1$: Monotonic linear dependence $\Gamma_Z(E_r)$ vanishes resulting on regions with weaker and enhanced inward flux.
- The **numerically** simulated flux level **agree reasonably well** with **analytical prediction**.
- To what extent moderation of inward (or even outward) $\Gamma_Z$ are expected when $E_r < 0$? $\rightarrow$ **comprehensive scans of plasma parameters**.

# Analytical results: the *mixed-collisionality* regime

In the *mixed collisionality regime*:

- When the main ions are low collisional and the impurities are in the Pfirsch-Schlüter regime:

$\rightarrow$ if $\varphi_1 = 0$ the dependence of $\Gamma_Z$ on $E_r$ vanishes. [Helander PRL'17] $\rightarrow$ more likely screening.

$\rightarrow$ if $\varphi_1 \neq 0$ the dependence of $\Gamma_Z$ on $E_r$ is recovered, even at low $\varphi_1$ values [Calvo NF'18, Buller JPP'18].

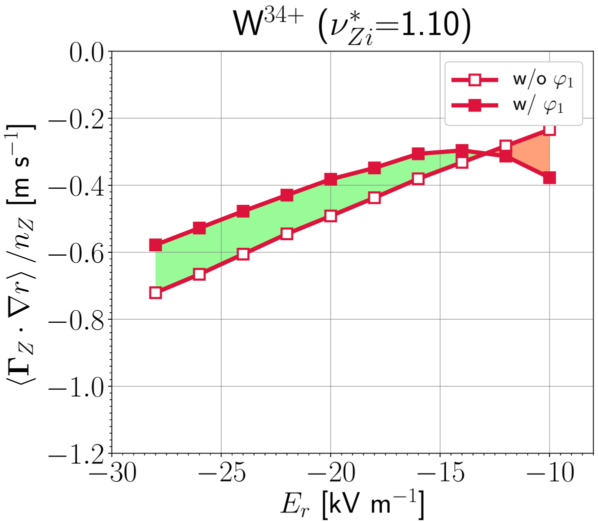


- w/o $\varphi_1$: The monotonic flux **dependence on** $E_r$ weakens, or equivalently $\Gamma_Z(E_r)$ flattens.
- w/ $\varphi_1$: Monotonic linear dependence $\Gamma_Z(E_r)$ vanishes resulting on regions with weaker and enhanced inward flux.
- The **numerically** simulated flux level **agree reasonably well** with **analytical prediction**.
- To what extent moderation of inward (or even outward) $\Gamma_Z$ are expected when $E_r < 0$? $\rightarrow$ **comprehensive scans of plasma parameters**.

In the *mixed collisionality regime*:

- When the main ions are low collisional and the impurities are in the Pfirsch-Schlüter regime:

$\rightarrow$ if $\varphi_1 = 0$ the dependence of $\Gamma_Z$ on $E_r$ vanishes. [Helander PRL'17] $\rightarrow$ more likely screening.

$\rightarrow$ if $\varphi_1 \neq 0$ the dependence of $\Gamma_Z$ on $E_r$ is recovered, even at low $\varphi_1$ values [Calvo NF'18, Buller JPP'18].

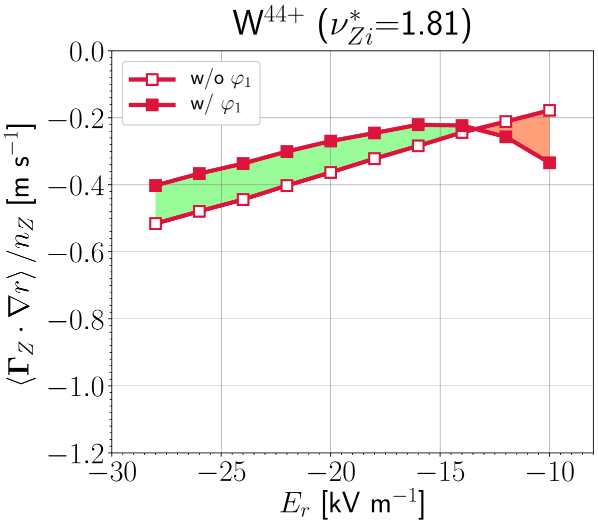


- w/o $\varphi_1$: The monotonic flux **dependence on** $E_r$ weakens, or equivalently $\Gamma_Z(E_r)$ flattens.
- w/ $\varphi_1$: Monotonic linear dependence $\Gamma_Z(E_r)$ vanishes resulting on regions with weaker and enhanced inward flux.
- The **numerically** simulated flux level **agree reasonably well** with **analytical prediction**.
- To what extent moderation of inward (or even outward) $\Gamma_Z$ are expected when $E_r < 0$? $\rightarrow$ **comprehensive scans of plasma parameters**.

In the *mixed collisionality regime*:

- When the main ions are low collisional and the impurities are in the Pfirsch-Schlüter regime:

$\rightarrow$ if $\varphi_1 = 0$ the dependence of $\Gamma_Z$ on $E_r$ vanishes. [Helander PRL'17] $\rightarrow$ more likely screening.

$\rightarrow$ if $\varphi_1 \neq 0$ the dependence of $\Gamma_Z$ on $E_r$ is recovered, even at low $\varphi_1$ values [Calvo NF'18, Buller JPP'18].

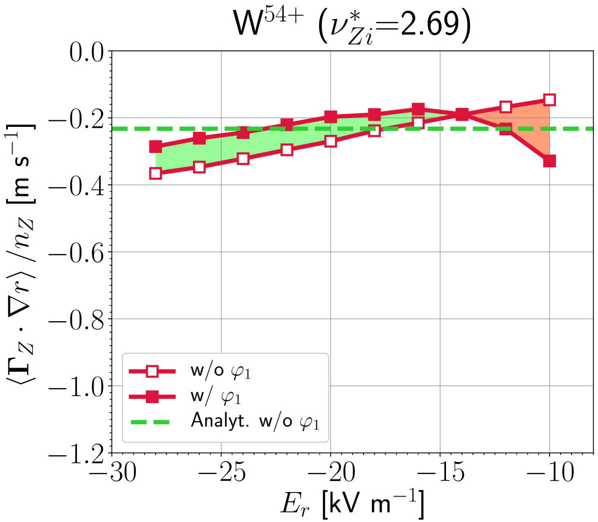


- w/o $\varphi_1$: The monotonic flux **dependence on** $E_r$ weakens, or equivalently $\Gamma_Z(E_r)$ flattens.
- w/ $\varphi_1$: Monotonic linear dependence $\Gamma_Z(E_r)$ vanishes resulting on regions with weaker and enhanced inward flux.
- The **numerically** simulated flux level **agree reasonably well** with **analytical prediction**.
- To what extent moderation of inward (or even outward) $\Gamma_Z$ are expected when $E_r < 0$? $\rightarrow$ **comprehensive scans of plasma parameters**.

- **Analytical formulas for $\Gamma_Z$** for trace impurities and large-aspect ratio in the mixed collisionality regime available in [Calvo NF'18, Buller JPP'19].
- Extended to include **main-ion pressure anisotropy** (III) for low $\nu_{*i}$ and different collisionality regimes for impurities in [Calvo arXiv: 1907.08482] (see **P1-05**).
- Formulas depend on the main ion distribution $h_i$, which need to be numerically worked out:

$$\boxed{\texttt{KNOSOS} \xrightarrow{h_i} \text{Analytical formulas for } \Gamma_Z}$$

- In W7-X (top), weaker $\varphi_1$ leads to $V_Z > 0$ for $\partial \log T_i/2 < \partial_r \log n_i$.
- In LHD (bottom), stronger $\varphi_1$ leads to $V_Z > 0$ restricted to $\partial_r \log n_i > 0$.

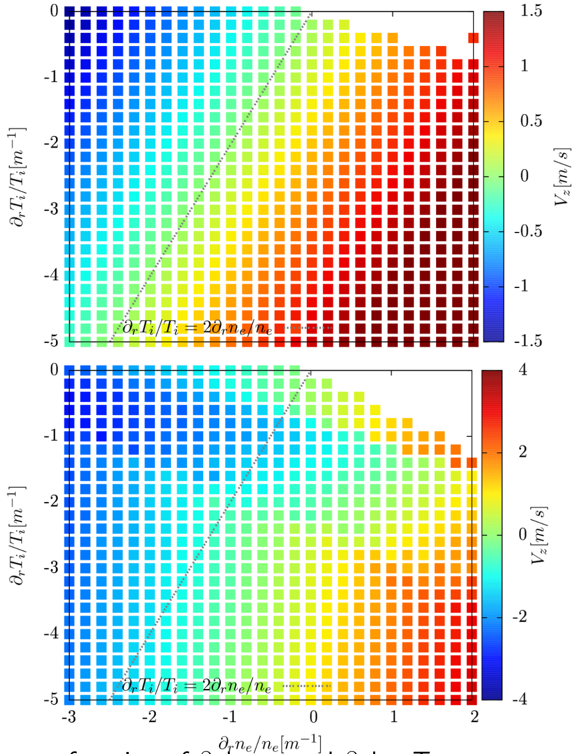


$V_{W^{44}}$ as function of $\partial_r \log n_i$ and $\partial_r \log T_i$.
$n_e = 6.3 \times 10^{19}$ m$^{-3}$, $T_b = 1.7$ keV. 600 runs.

- The impurity hole plasma simulated with SFINCS [Mollén PPCF'18] (exact F-P collision operator, multispecies (at non-trace concentration), including $\varphi_1$ yields:
- **Huge corrections** to standard neoclassical calculations.
- Impact goes in the opposite direction to what experiment indicates (**inward $\Gamma_Z$ considerably enhanced**).

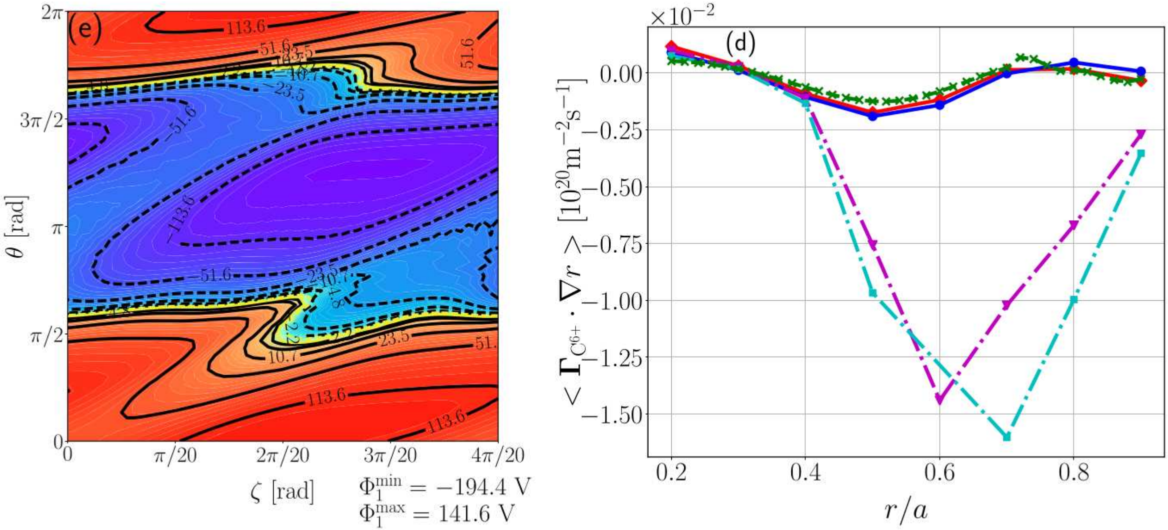


F-P w/o $\varphi_1$; PAS w/o $\varphi_1$ ; **F-P w/** $\varphi_1$ ; PAS w/ $\varphi_1$; **DKES + momentum conserv.**

# Experimental characterization of $\Phi_1$ in TJ-II

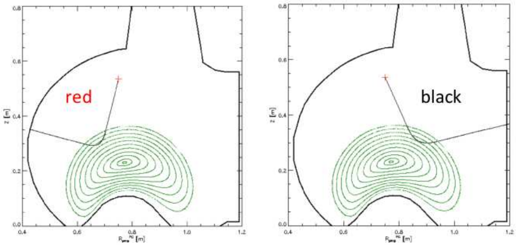


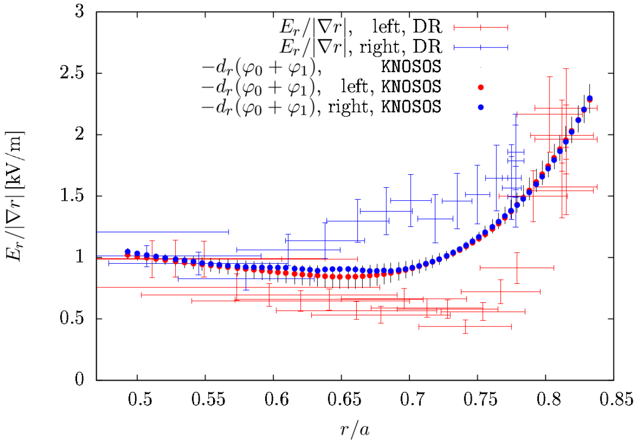


- Past experiments have measured differences on plasma potential attributable to $\Delta\varphi_1$ [Pedrosa NF'15].
- Doppler reflectometry (DR) has measured at different poloidal and toroidal positions appreciable difference on the total radial electric field [Estrada NF'19].
- Contribution from $-\mathrm{d}\Phi_1/\mathrm{d}r$ to the total radial electric field calculated with `EUTERPE` [Regaña PPCF'18] and `KNOSOS` .
- **Radial electric field contribution from** $-\mathrm{d}_r\varphi_1$ is negligible with adiabatic electrons.
- **Including kinetic electrons** matters and $-\mathrm{d}_r\varphi_1$ correction become appreciable althought not to the level the DR system observes.

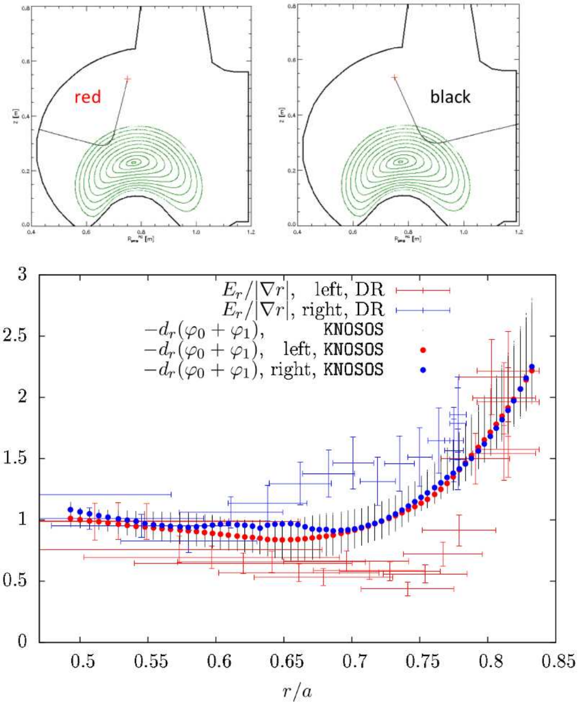


- Past experiments have measured differences on plasma potential attributable to $\Delta\varphi_1$ [Pedrosa NF'15].
- Doppler reflectometry (DR) has measured at different poloidal and toroidal positions appreciable difference on the total radial electric field [Estrada NF'19].
- Contribution from $-\mathrm{d}\Phi_1/\mathrm{d}r$ to the total radial electric field calculated with `EUTERPE` [Regaña PPCF'18] and `KNOSOS` .
- **Radial electric field contribution from** $-\mathrm{d}_r\varphi_1$ is negligible with adiabatic electrons.
- **Including kinetic electrons** matters and $-\mathrm{d}_r\varphi_1$ correction become appreciable althought not to the level the DR system observes.

# $\Gamma_Z$ in W7-X#180919.055

- Numerical analyses of W7-X discharges have recently been approached with these tools.
- The agreement between the codes is found where they are expected to agree.
- The differences between SFINCS and EUTERPE on $\varphi_1$ or collision operator translate into small difference on neoclassical fluxes.

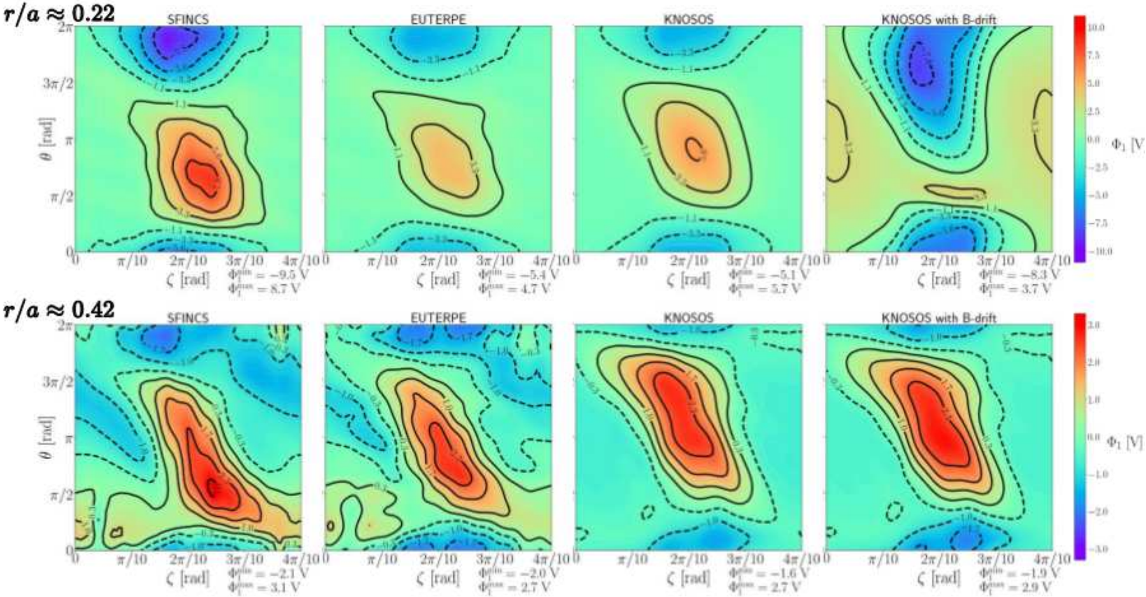

- Numerical analyses of W7-X discharges have recently been approached with these tools.
- The agreement between the codes is found where they are expected to agree.
- The differences between SFINCS and EUTERPE on $\varphi_1$ or collision operator translate into small difference on neoclassical fluxes.

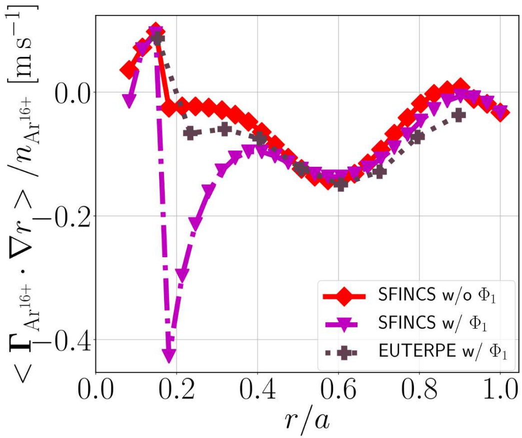


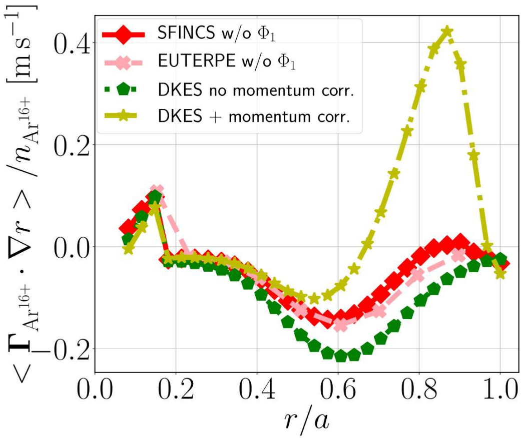

- Numerical analyses of W7-X discharges have recently been approached with these tools.
- The agreement between the codes is found where they are expected to agree.
- The differences between SFINCS and EUTERPE on $\varphi_1$ or collision operator translate into small difference on neoclassical fluxes.

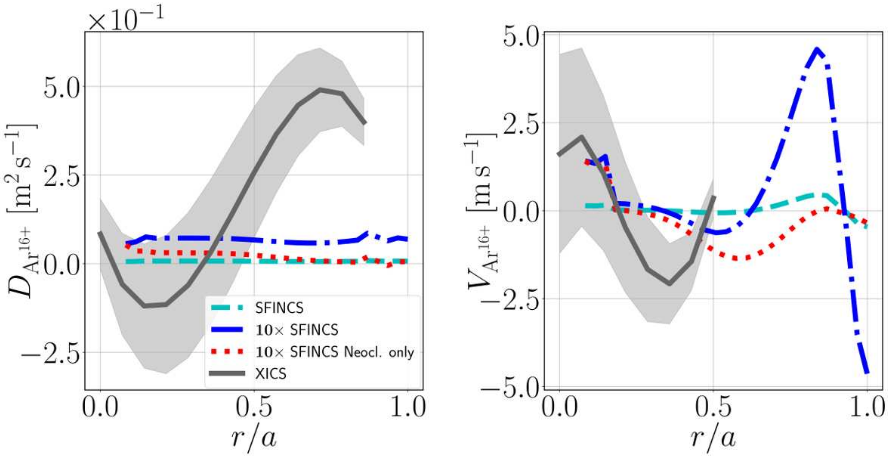


- $D_{Ar^{16+}}$ is strongly underestimated. XICS-measured $V_Z$ and neoclassical estimate coincide in sign, but disagree in a factor of O(10).
- Including **classical flux**, which can be **important in W7-X** [Buller JPP'19], strongly modifies $V_Z$ in the mid outer regions → to what extent the difference on $V_Z$ and $D_Z$ are attributtable to turbulence?

## Code characteristics

- Eulerian + semi-Lagrange, delta-f nonlinear gyrokinetic code.
- Mixed implicit-explicit scheme.
- Multiple ion species + kinetic electrons.
- General nested flux surface geometry (including interface with VMEC).
- Currently flux tube, full flux surface under development.
- Benchmarked against GS2. Ongoing stellarator specific benchmark against GENE.
- Coupled to SFINCS for neoclassical equilibrium and $\varphi_1$ (coupling with KNOSOS foreseen).

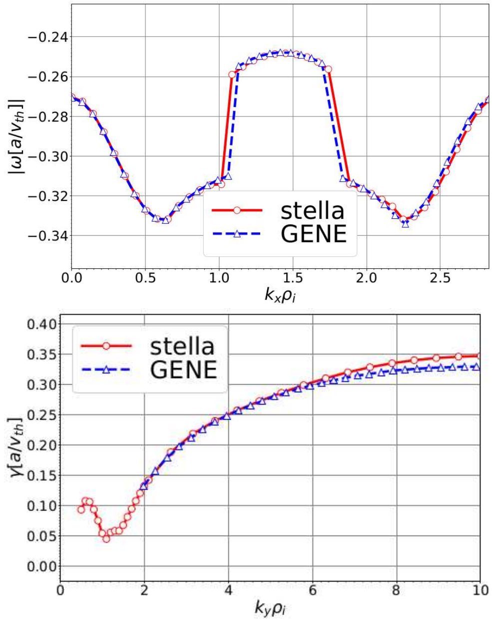


Selected stella /GENE benchmark results: frequency $\omega(k_x)$ for an ITG case w/ adiabatic e$^-$ (top); growth rate $\gamma(k_y)$ for a TEM case (bottom) [A. G. Jerez *in progress*.]

[1] M. Barnes, F. I. Parra and M. Landreman J. Comput. Phys. (2019)

- In the trace impurity limit it can be written a transport law of the form:

$$\Gamma_Z^{\mathrm{ql}} = -n_Z \left( D_{Z1} \frac{\mathrm{d} \ln n_Z}{\mathrm{d} r} + D_{Z2} \frac{\mathrm{d} \ln T_Z}{\mathrm{d} r} + C_Z \right),$$

- For sufficiently heavy impurities, with bounce ($\omega_{bZ}$) and drift ($\omega_{dZ}$) frequencies, in the presence of an instability with fluctuating potential $\phi$, frequency $\omega$ and $k_\perp \rho_i \lesssim 1$:

$$\omega/\omega_{bZ} \gg 1 \quad \text{and} \quad \omega/\omega_{dZ} \gg 1.$$

- Then, the solution of the GK eq. for the impurity distribution function $g_Z$ leads to:

$$D_{Z1} = \frac{\gamma k_\alpha^2}{\omega^2 + \gamma^2} \left\langle \phi^2 \Gamma_0(b) \right\rangle$$

$$D_{Z2} = \frac{\gamma k_\alpha^2}{\omega^2 + \gamma^2} \left\langle \phi^2 b \left[ \Gamma_1(b) - \Gamma_0(b) \right] \right\rangle$$

$$C_Z = 0$$

with $b = k_\perp^2 T_Z / m_Z \Omega_Z^2$, $\Gamma_n(b) = I_n(b) e^{-b}$.

- Accounting for the specific $\phi$ structure, growth rate, frequency, magnetic geometry, parallel impurity dynamics (not included in analytical treatment) requires a numerical approach.
- Collisions are not included.
- W7-X (std. config.), $r/a = 0.8$ with $T_i = T_e = 0.5$ keV, $a/L_{T_i} = a/L_{T_e} = 6.0$ and $a/L_{n_i} = a/L_{n_e} = 1.0$.

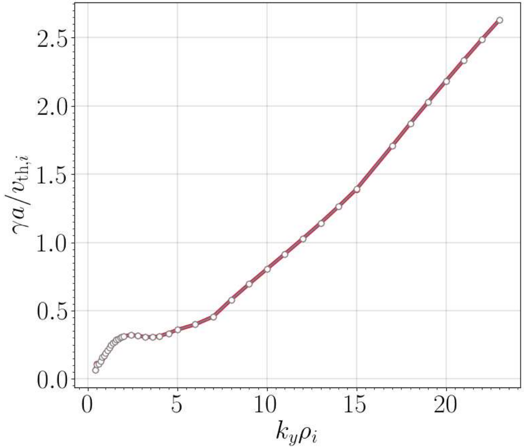


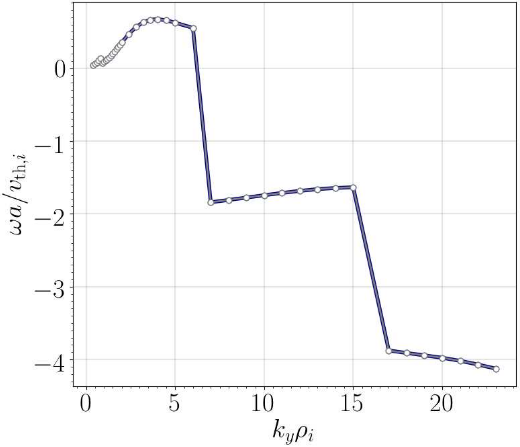


- The calculated impurity radial flux of a linear GK simulation ($\Gamma_Z$) allows, defining $\Gamma_Z^{\mathrm{ql}}$ as:

$$\Gamma_Z^{\mathrm{ql}} = \Gamma_Z \frac{\omega^2 + \gamma^2}{\gamma k_y^2 \langle \phi^2 \rangle},$$

to work out the spectra, relative sizes and sign of $D_{Z1}$, $D_{Z2}$ and $C_Z$[1].

[1] For characterizing LHD impurity hole plasma see [Mikkelsen PoP'14].

# Quasilinear transport of impurities with stella

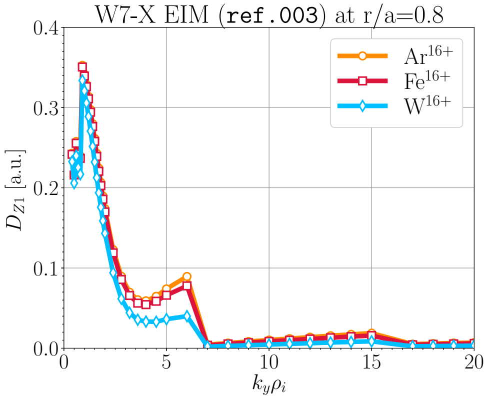


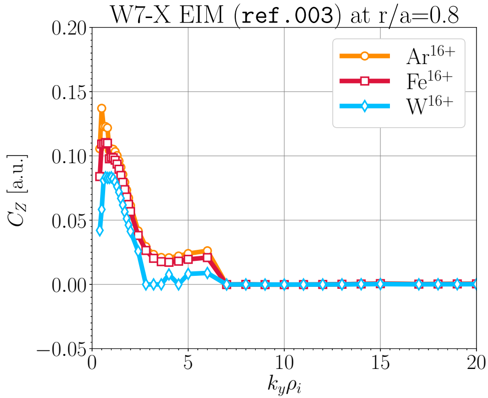


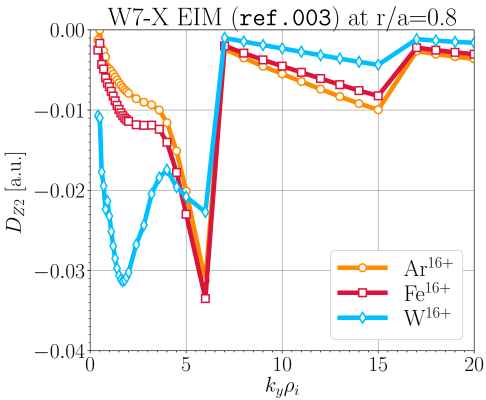


- $D_{Z1} \Rightarrow$ **outward-directed** $\Gamma_Z^{ql}$ while $D_{Z2} \Rightarrow$ (much weaker) **inward-directed** $\Gamma_Z^{ql}$.
- Covection term $C_Z$ introduces additional **inward-directed** $\Gamma_Z^{ql}$ contribution.
- Weak mass or $Z$-dependence observed [Barnes PRL'12], with the exception of the $D_{Z2}$ at low $k_y$.
- $\Gamma_Z^{ql}$ abruptly decreases once the electron-driven (ETG) instability is found at $k_y\rho_i > 6$.

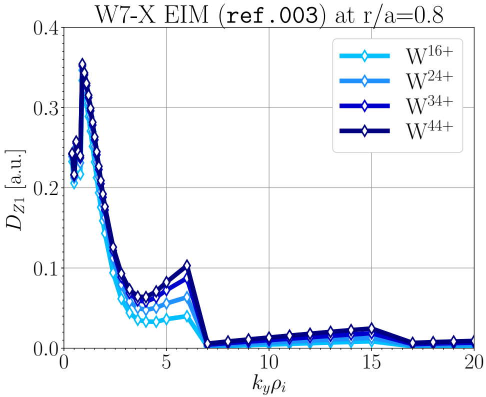


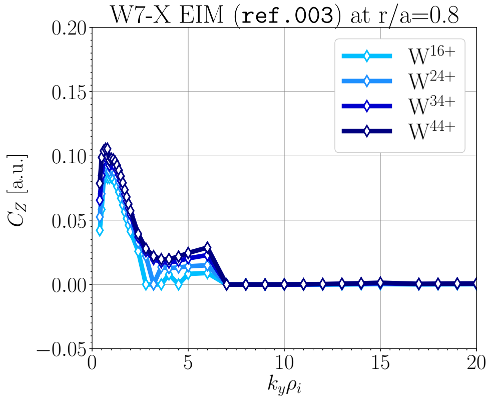


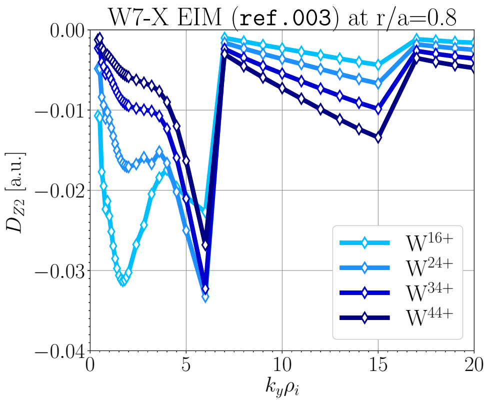


- $D_{Z1} \Rightarrow$ **outward-directed** $\Gamma_Z^{ql}$ while $D_{Z2} \Rightarrow$ (much weaker) **inward-directed** $\Gamma_Z^{ql}$.
- Covection term $C_Z$ introduces additional **inward-directed** $\Gamma_Z^{ql}$ contribution.
- Weak mass or $Z$-dependence observed [Barnes PRL'12], with the exception of the $D_{Z2}$ at low $k_y$.
- $\Gamma_Z^{ql}$ abruptly decreases once the electron-driven (ETG) instability is found at $k_y\rho_i > 6$.

- Preliminary **nonlinear analyses** have begun.
- W7-X (std. config.) at $r/a = 0.8$ with $T_i = T_e = 0.5$ keV, $a/L_{T_i} = 6.0$ and $a/L_{n_i} = 1.0$. adiabatic electrons:

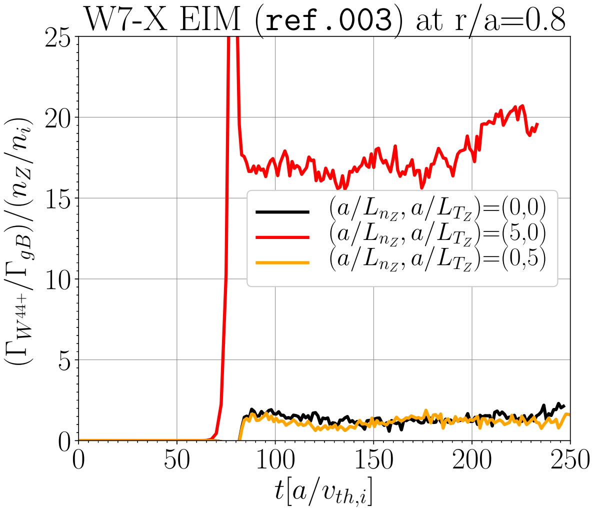


| | Quasilinear | Nonlinear |
|---|---|---|
| $D_{Z1}$=$D_Z$ | $> 0$ | 1.6 |
| $D_{Z2}$ | $< 0$ | -0.02 |
| $C_Z$ | $> 0$ | -1.38 |
| $V$ | $< 0$ | 1.1 |

$[D_Z]$=$\Gamma_{gB} n_i^{-1}$m ; $[C_Z]$=$[V]$=$\Gamma_{gB} n_i^{-1}$.

- Nonlinear simulations show (and QL analyses capture too) **strong outward-directed** $n'_Z$-driven diffusion, and **weak** inward-directed thermo-diffusion.
- Nonlinearly **anti-pinch** ($C_Z$) is found, which contradicts QL analysis.

## Summary

- The basic understanding of collisional impurity radial transport has improved due to an intense code and analytical theory development in recent years.

| | EUTERPE [2] | SFINCS | KNOSOS + analyt. $\Gamma_Z$ | FORTEC-3D |
|---|---|---|---|---|
| Kind | Monte-Carlo $\delta f$ | Eulerian $\delta f$ | Bounce-averaged $\delta f_i$ | Monte-carlo $\delta f_i$ |
| Geometry | General/VMEC | General/VMEC | General/VMEC | General/VMEC |
| Local/global | Local | Local | Local | Global |
| $\mathbf{v}_m \cdot \nabla\alpha^\dagger$ | None | Model | Analytically exact. | Included |
| C(f) for $Z$ | $\sqrt{m_i/m_Z}$-expanded[3] | Linearized Fokker-Planck | Analy. eval. $\Gamma_Z$ | Model for $C_{ab}$ |
| C(f) for i,e | Model for $C_{aa}$ | Exact Fokker-Planck | PAS [4] | Model for $C_{ab}$ |
| CPU usage | Intense | Moderate/intense | Light | Intense |

- The benchmark work has quantitatively confirmed the impact of neoclassical effects, traditionally neglected, that are important for an accurate evaluation of neoclassical $\Gamma_Z$.
- Experimental confirmation of predictions has been moderate (e.g. $\varphi_1$ measurements, of convection $V_Z$ in selected LHD plasmas) but also made evident big gaps, for instance, $D_Z$.
- First quasilinear and nonliner simulations carried out in order to study the role of gyrokinetic turbulence on $\Gamma_Z$.

[2] Neoclassical version of the code EUTERPE

† Tangential magnetic drift. Necessary for $E_r \ll T/(ea)$, when superbanana plateau regime is accessed [Calvo PPCF'17].

[3] w/o pressure anisotropy terms.

[4] Pitch angle scattering.

# Backup slides

- Expressing the flux in terms of the conventional diffusion and convection coefficient $D_Z$ and $V_Z$:

$$\frac{\Gamma_Z^{\mathrm{ql}}}{n_Z} = -D_Z \frac{\mathrm{d} \ln n_Z}{\mathrm{d}r} + V_Z$$

$V_Z$ can be obtained for a specific value of $T_Z'$. Setting $a/L_{T_Z} = a/L_{T_i} = -6.0$ yields:

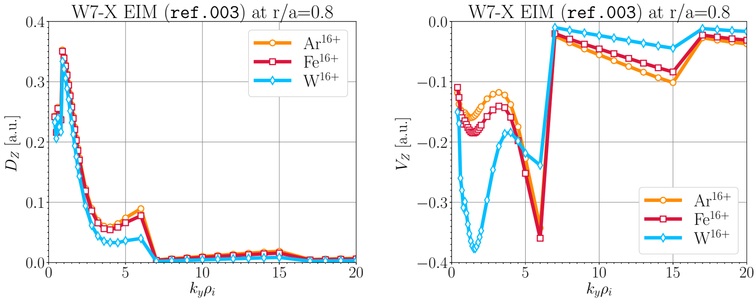

- Expressing the flux in terms of the conventional diffusion and convection coefficient $D_Z$ and $V_Z$:

$$\frac{\Gamma_Z^{\mathrm{ql}}}{n_Z} = -D_Z \frac{\mathrm{d}\ln n_Z}{\mathrm{d}r} + V_Z$$

$V_Z$ can be obtained for a specific value of $T_Z'$. Setting $a/L_{T_Z} = a/L_{T_i} = -6.0$ yields:

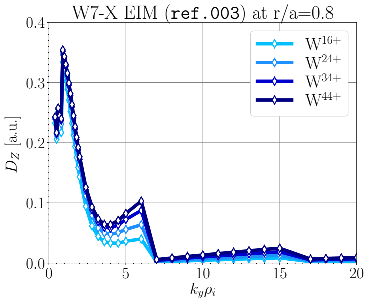


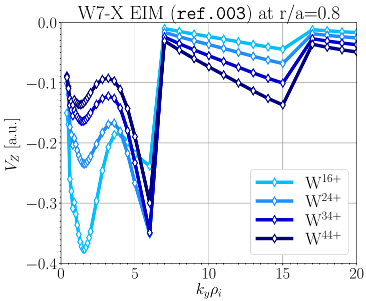


- $V_Z$ and $D_Z$ have opposite sign, which would lead to peaked $n_Z$ profiles.
- $V_Z$ and $D_Z$ have comparable size, which conflicts with the conclusion about $V_Z$ and $D_Z$ set by different mechanisms (NC or turb.) given their calculated values.